DEPOSITION AND CHARACTERIZATION OF ANTIMONY SELENIDE THIN FILMS

A. U. Bajpeyee
Department of Physics, Arts, Science and Commerce College,
Kiran Nagar, Amravati 444606, Maharastra (INDIA)

(*Received : 18.03.2012; Revised : 04.05.2012; Accepted : 08.06.2012*)

Abstract
Cost-effective solar cells can be prepared from the semiconducting Sb2Se3 thin films. These are the thin films with polycrystalline absorbing nature used for solar cells. The aim of this article is to study and prepare Sb2Se3 film by using simple chemical bath technique. The films were characterized by using X-ray diffraction (XRD), ultraviolet-visible spectro-photometer (UV/Vis). The nano-crystalline nature of the Sb2Se3 films is calculated and confirmed to be 26 nm. The activation energy estimated is 0.78 eV and the optical direct band gap value estimated is 1.65 eV at room temperature.
Keywords:-Cost-effective,Sb_2Se_3,Chemical ,

1. Introduction

Antimony selenide (Sb2Se3) is an attentive material due to its switching, photovoltaic, thermoelectric, optical and electrical properties [1, 2]. Various methods have been in use to synthesize Sb2S3 semiconductor, such as single-source precursor [3], electro-deposition [4], high temperature evaporation [5, 6], solvo-thermal [7] methods. As a direct band gap of 1.3 eV energy semiconductors, Sb2S3 exhibits photovoltaic and thermoelectric properties, which make it potential in solar selective and decorative coating, optical and thermoelectric cooling devices [8], compositional deposition methods affect these properties [9, 10]. With this band gap energy of antimony selenide (Sb2S3) semiconductor films absorbs low energy light in a visible and near-infrared region. The use of Sb2S3 semiconductor as a thin film was of basic interest to improve efficiency and stabilities in solar cells [11, 12]. The optical storage based on the amorphous crystalline phase transition of it has been studied [13]. A few reports of Sb:Se thin films in solar cells is noticed [14]. Among several methods, economical is chemical bath technique and is noticeable due to its simplicity and cost. Hence, reported.

2. Materials and Method

Sb2Se3 thin films were prepared from ionic forms of basic precursors into fresh double distilled water. Chemicals used were from Merck (India) 99% pure and are antimony potassium tartarate [K(SbO)C4H4O6] and sodium seleno-sulphate (Na2SeSO3). The 0.1 molar Na2SeSO3 after mixing in 1:10 proportion of selenium powder with anhydrous sodium sulfite at constant stirring for 12 h at 80˚C. Obtained clear solution of Na2SeSO3, 0.5M antimony potassium tartarate solution was added with 0.1M ammonia solution slowly to form complex at the pH level 9 and radish brown solution of which Sb2Se3 thin films were formed on glass substrates at room temperature. The substrates coated with Sb2Se3 was removed after 1.5 h and rinsed with de-ionized water, dried in air. Adherent films to the substrate give maximum thickness of 280 nm. As-deposited annealed Sb2Se3 films at 100oC, 200oC, 300oC, 400oC and 500oC were characterized further. Reaction mechanism in alkaline medium is

hydrolysis of sodium seleno-sulphate which gives Se2- ions as,

$Na_2SeSO_3 + OH^- \rightarrow Na_2SO_4 + H Se^-$

$H Se^- + OH^- \rightarrow H_2O + Se^{2-}$

The Sb^{3+}ions react with Se^{2-} ions in the reaction bath to give Sb_2Se_3 film formation: $2Sb^{3+} + 3Se^{2-} \rightarrow Sb_2Se_3 \downarrow$

The films were structurally characterized by X-Ray diffraction (Cu-Kα radiations) and ultraviolet-visible spectro-photometer (UV/Vis); the thermal activation energy is also calculated in the laboratory set up.

3. Structural and Electrical Studies

3.1 X-ray diffraction (XRD) Study

X-ray diffraction (XRD) studies were carried out for the as deposited Sb_2Se_3 thin films on glass substrates annealed at the temperatures 100oC, 200oC, 300oC, 400oC and 500oC. It revealed nano-crystalline to polycrystalline phase transition. Figure 1 shows XRD patterns of Sb_2Se_3 films, with poor crystallinity. The peak intensity increases with annealing temperature. The XRD pattern shows broadness indicating the films on the amorphous substrate. XRD patterns were compared and confirmed from standard JCPDS data card file 15-0861 [15]. From it, single orthorhombic single phase is matched and indexed accordingly. The average crystallite size of Sb_2Se_3 is calculated by Debye Scherer's formula (1),

$$d = \frac{0.9\lambda}{\beta \, Cos\, \theta} \text{ ----------(1)}$$

where, λ is wavelength of X-ray, θ is Bragg's diffraction angle and ß is full width at half maximum intensity of diffraction peak. Crystalline size of Sb_2Se_3 thin film increases with annealing. It in average is 26 nm and increases from 14 nm to 40 nm as annealing temperature increases.

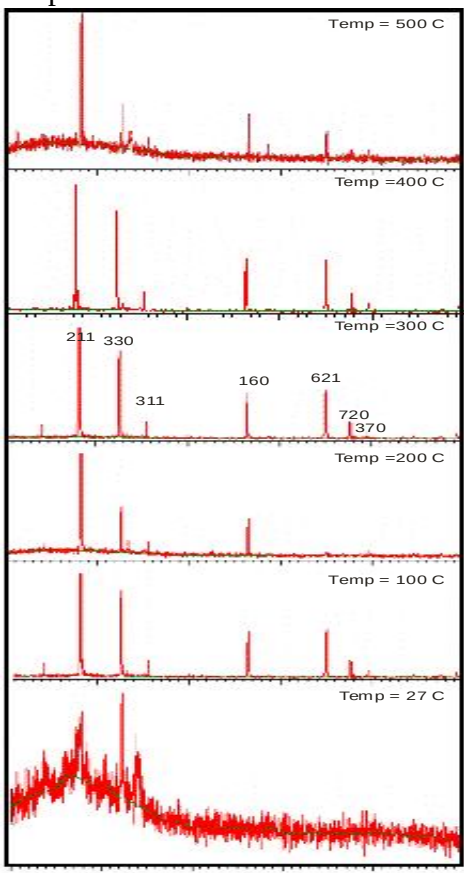

Figure 1: Indexed XRD patterns of Sb_2Se_3 thin films

3.2 Electrical Resistivity and Activation Energy

Variation of dc-electrical resistivity with temperature is studied for the Sb_2Se_3

films annealed at different temperatures. Figure 2 shows the variation of log (ρ) with reciprocal of temperature for as deposited and annealed films. The decrease in resistivity with increase in temperature confirms the semiconducting nature of the films. The decrease in resistivity with increase in annealing temperature may be due to improvement in crystal structure.

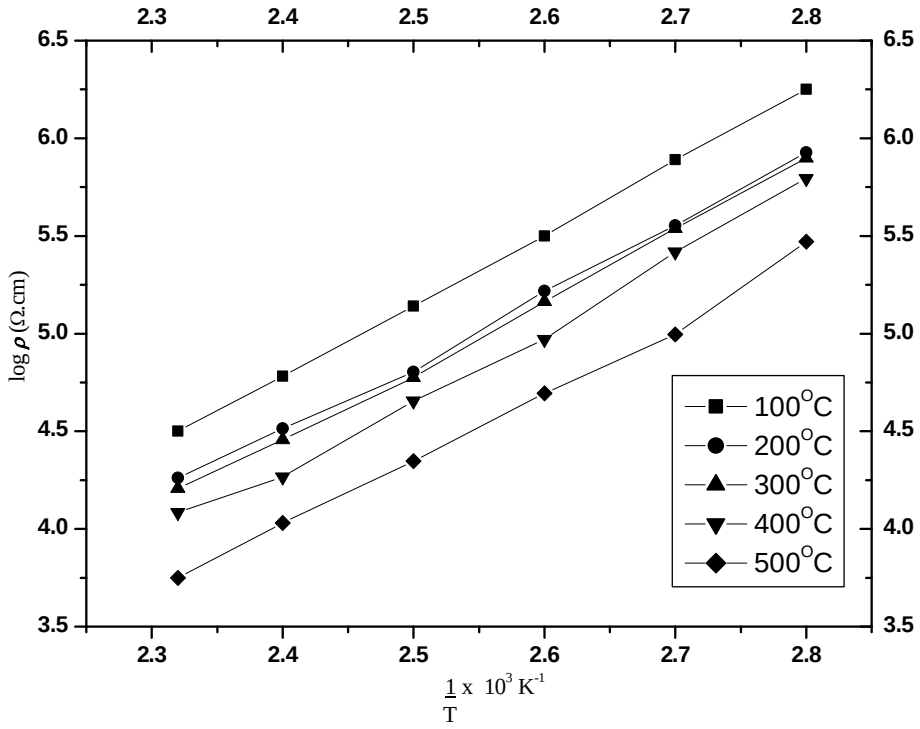

Figure 2: Sb2Se3 thin films: log of resistivity vs reciprocal of temperature

The approximate straight lines in the log ρ vs 1000/T plot indicates temperature independence of resistivity suggesting acoustical mode lattice scattering [16]. By using the calculated slope of the graph of log (ρ) with temperature and the activation energy (ΔE) is calculated by using the formula (2)

ΔE = {slope x K}/{1.6 x 10-19} eV ---------- (2)

Where, K is Boltzmann's constant, K=1.380 x 10-23 J/K

The activation energy depends on the annealing temperature of the film. The activation energy decreases with increase in annealing temperature which is independent at higher and lower annealing temperatures. Figure 3 shows variation in activation energy from 0.78 to 0.59 eV with annealing temperature from 270C to 5000C. This may due to the change of crystal structure and the usual thermal rise as in hoping of electrons between localized defect states by transport through atomic sites [17].

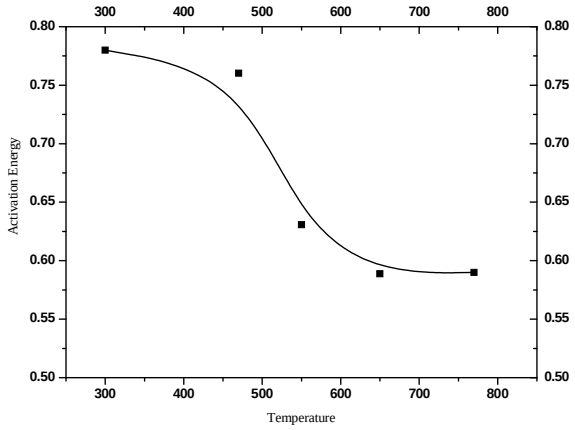

Figure 3: Variation of activation energy (eV) of Sb2Se3 film with annealing temperature.

3.3 Optical Absorption Studies

Optical absorption may help in explaining some features concerning the band structure of materials. Here, optical absorption in Sb2Se3 films was carried out within the wavelength range 300 of 1100 nm. Figure 4 shows optical absorption curves for Sb2Se3 films annealed at different temperatures. For allowed direct transition the plots of (αhυ)2 vs hυ are shown in figure 5

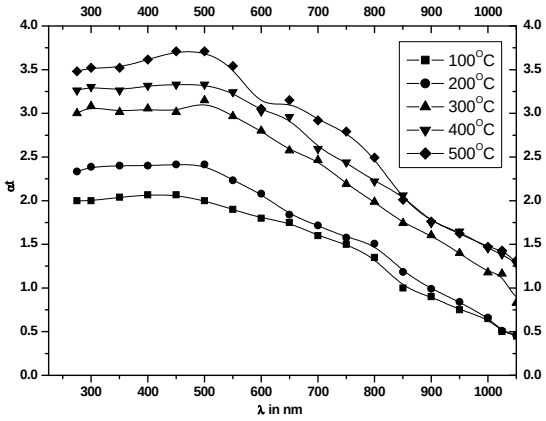

Figure 4: optical absorption (αt) against wavelength (λ) of Sb2Se3 thin films

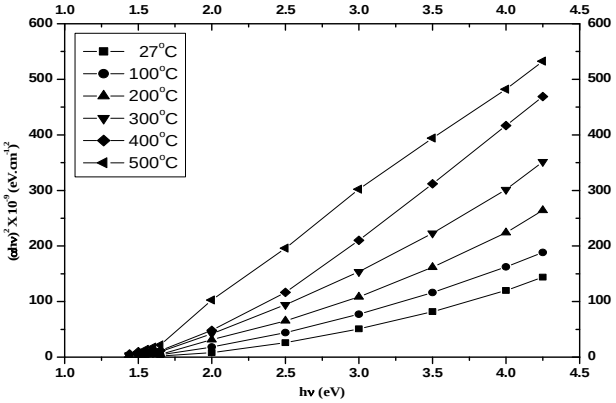

Figure 5: (αhυ)2 vs hυ for Sb2Se3 thin films

Since the plots of (αhυ)2 against hυ are almost linear, the direct nature of the optical transition in Sb2Se3 is confirmed. At zero absorption coefficient the direct optical energy gaps (Eg) decreases from 1.65 eV to 1.44 eV when annealed from room temperature to 500oC for one hour. This decrease in Eg is mainly attributed to improve grain size of the film after annealing and agrees with the behavior shown for different annealed films [18, 19].

4. Conclusions

Structural, electrical and optical aspects with respect to XRD for Sb2S3 thin films deposited on glass substrate for varying annealing temperatures is successfully studied. XRD confirms nano-crystallite size between 14-40 nm along with orthorhombic phase. The observations at room temperature as activation energy of the film 0.78 eV and the optical direct band gap value 1.65 eV were recorded.

Acknowledgements

I acknowledge Panjab University (India) for XRD facilities. Also to Prof. Dr. B. H. Pawar, Dr. G. N. Chaudhari and Dr. F. C. Raghuwanshi for active guidance.

References:

N.S. Platakis, H.C. Gatos, Phys. Status Solidi A 13 (1972) K1.

K.Y. Rajapure, C.D. Lokhande, C.H. Bhosele, Thin Solid Films 311 (1997) 114.

J. Yang, J.H. Zeng, S.H. Yu, L. Yan, Y.H. Zhang, Y.T. Qian, Chem. Mater. 12 (2000) 2924.

J.C. Bao, C.Y. Tie, Z. Xu, Z.Y. Suo, Q.F. Zhou, J.M. Hong, Adv. Mater. 20 (2002) 1483.

Z.W. Pan, Z.R. Dai, Z.L. Wang, Science (Washington, DC) 291 (2001) 1947.

Z.R. Dai, J.L. Gole, J.D. Stout, Z.L. Wang, J. Phys. Chem. B 106 (2002) 1274.

M.S. Mo, J.H. Zeng, X.M. Liu, W.C. Yu, S.Y. Zhang, Y.T. Qian, Adv. Mater. 14 (2002) 1658.

K. Rajapure, C. Lokhande, C. Bhosele, Thin Solid Films 311 (1997) 114.

A.M. Fernandez, M.G. Merino, Thin Solid Films 366 (2000) 202-206

D. Bransen, Non-Cryst. Solids 15 (1974) 395

P. Pramanik, et al. *J. Solid. Chem.* **1982,** 44**,** 425.

Y. Rodrigues-Lazcano, et al. *Thin solid films* **2005,** 493, 77-82.**] K. Watanabe, N.**

Sato, S. Miyaoka, J. Appl. Phys. 54 (1983) 1256.

C. Kaito, T. Fujita, T. Kimura, et al., Thin Solid Films 312 (1998) 93.

J. Dikova, V. Mankov and N. Starbov, vacuum 47/12 (1996)1487. **] L.R.**

Gillbert, B. Xan Pelt and C. Wood J. Phys. Chem. Solids 35(1994)1629.

F. Abd EI–Salam, M. A. Afify and E. Abd EI-Wahabb, vacuum 2 (1993) 111.

G. Hodes, A.A. Xaron, F Decker, P. Motosuke, Phys. Rev. B 36 (1987) 4214.
[19**] G. Hodes,** Phys. Chem. Chem. Phy. 9 (2007) 2181.